Broadband Least-Squares Wave-Equation Migration

Shaoping Lu
PGS
West Memorial Place I
15375 Memorial Drive, Suite 100
Houston, TX 77079, USA
Shaoping.Lu@pgs.com

Alejandro Valenciano
PGS
West Memorial Place I
15375 Memorial Drive, Suite 100
Houston, TX 77079, USA
Alejandro.Valenciano@pgs.com

Nizar Chemingui
PGS
West Memorial Place I
15375 Memorial Drive, Suite 100
Houston, TX 77079, USA
Nizar.Chemingui@pgs.com

Andrew Long*
PGS
Level 4, IBM Centre
1060 Hay Street
West Perth, WA 6005, Australia
Andrew.Long@pgs.com

SUMMARY

We introduce an effective iterative Least-Squares Wave-Equation Migration (LS-WEM) solution for broadband imaging. Least-Squares Migration (LSM) solutions are designed to produce images of the subsurface corrected for wavefield distortions caused by acquisition and propagation effects. They implicitly solve for the earth reflectivity by means of data residual reduction in an iterative fashion, which usually demands intensive computation. The LS-WEM is implemented using a visco-acoustic anisotropic one-way wave-equation wavefield propagator that is able to fully utilize both the broader seismic bandwidth and the high-resolution velocity information from Full Waveform Inversion (FWI). Our implementation combines the one-way extrapolator with fast linear inversion solvers into an efficient migration inversion system.

Application to the 2D Sigsbee2b synthetic model improves the sub-salt illumination by balancing the image amplitudes and reducing the effects of the shadow zones, enhances temporal resolution by broadening the frequency spectrum, balances the wavenumber content and improves images of faults and dipping salt flanks. In addition, LS-WEM converges rapidly to the true solution, reducing the data residuals by 90% in only four iterations. Application to real 3D datasets from the Gulf of Mexico and the North Sea demonstrates high-resolution imaging with reduced acquisition footprint effects, improved spatial frequency content, and better structural imaging at all depths.

Key words: Migration, inversion, acquisition footprint, illumination, wavenumber.

INTRODUCTION

Depth migration produces a blurred representation of the earth reflectivity, with biased illumination and limited wavenumber content. The image resolution at a given depth is controlled by the migration operators, the acquisition parameters (source signature, frequency bandwidth, acquisition geometry), and the earth properties at the reflector depth and the overburden (velocity, attenuation). Some of these conditions can be mitigated during acquisition and processing by employing technologies like: multi-sensor data, full azimuth acquisition geometries, deghosting, attenuation compensation and using high-resolution earth models during depth migration (i.e. models derived from Full Waveform Inversion). However, when heterogeneities are present in the earth and the acquisition geometry leads to insufficient source and receiver coverage on the surface, both the illumination and wavenumber content of the depth-migrated images can be significantly restricted.

The resolution of the depth images can be improved by posing the imaging problem in terms of least-squares inversion. Least-Squares Migration (LSM) solutions (Schuster, 1993; Nemeth et al., 1999; Prucha and Biondi, 2002) are designed to produce images of the subsurface corrected for wavefield distortions caused by acquisition and propagation effects. They implicitly solve for the earth reflectivity by means of data residual reduction in an iterative fashion, which usually demands intensive computation. In the seismic exploration framework, Nemeth et al. (1999) derived a LSM following a high-frequency Kirchhoff integral asymptotic approximation (ray-based). Later, Prucha and Biondi (2002) derived less restrictive broadband wave equation solutions. The advantage of broadband wave-equation extrapolators is that they make better use of the high-resolution earth models derived with advanced processing technologies such as Full Waveform Inversion (FWI: Korsmo et al., 2017).

Here, we implement an LSM using an accurate visco-acoustic anisotropic one-way wave-equation operator (Valenciano et al., 2011). Our application integrates the one-way operator with a fast linear inversion solver in an efficient migration/demigration workflow, namely a Least-Squares one-way Wave-Equation Migration (LS-WEM). Applications of LS-WEM to both synthetic and field data examples improve images amplitude balance and enhancements to both temporal and spatial resolution.

METHOD AND RESULTS

Seismic migration is the adjoint solution to the forward modeling problem:

$$\boldsymbol{m} = \boldsymbol{L}^T \boldsymbol{d}_{obs} \qquad (1)$$

where, $\boldsymbol{d}_{obs}$ is the observed data, $\boldsymbol{L}$ represents the linearized (Born) modeling operator, and its adjoint $\boldsymbol{L}^T$ is the migration operator. However, the heterogeneity of the overburden and/or limitations of the acquisition geometry can affect the illumination and wavenumber content of the estimated image $\boldsymbol{m}$.

A better approximation of the earth reflectivity is obtained by using a least-squares inversion, which solves a minimization problem to approximate the true reflectivity $\boldsymbol{m}$ as:

$$\boldsymbol{m} = \boldsymbol{argmin} \frac{\mathbf{1}}{\mathbf{2}} \|\boldsymbol{d}_{obs} - \boldsymbol{L}\boldsymbol{m}\|_2^2 \qquad (2)$$

In this case, the acquisition geometry, which relates to the operator $\boldsymbol{L}$, has less effect to the resulting image $\boldsymbol{m}$.

Here we introduce an implicit method to solve the least-squares problem. The LSM simulates data by wave-equation Born modeling, and iteratively updates the reflectivity by migration of the misfits between the observed and simulated data. The algorithm can be summarized by the diagram in Figure 1 using an iterative modeling/migration framework. The first step of the flow is to produce an approximate reflectivity (migration). In the next step, the reflectivity is used in Born modeling. When the data residual $\|\mathbf{d}_{obs} - \mathbf{d}_{mod}\|$ is large it is migrated to update the image $\boldsymbol{m}$. The inversion converges when the simulated data matches the observation. One iteration (blue loop in Figure 1) comprises one Born modeling step and one migration.

The computational cost of the iterative LSM relies on the efficiency of the wavefield propagation algorithm. Here we implement the inversion using a one-way wave-equation operator (Valenciano *et al.*, 2011) that has advantages of both accuracy and efficiency. In addition, our implementation combines the one-way extrapolator with fast linear inversion solvers into an efficient migration inversion system.

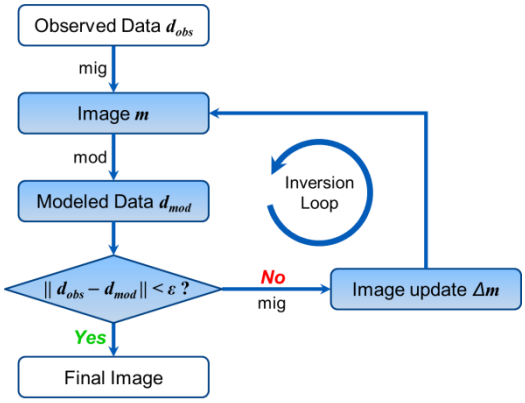

Figure 1: An iterative LSM algorithm solves for the earth reflectivity **m**. It simulates synthetic data $\mathbf{d}_{mod}$ by using a Born modeling operator, and iteratively update the reflectivity image **m** using migration of the data residual $\|\mathbf{d}_{obs} - \mathbf{d}_{mod}\|$.

SYNTHETIC AND FIELD DATA EXAMPLES

We have applied LS-WEM to the 2D Sigsbee2b synthetic model (Figure 2). The migration result (Figure 2A) shows uneven illumination from left to right where sediments transition to a subsalt area, including shadow zones related to the complex salt structures. LS-WEM improves the illumination by balancing the image amplitudes and reducing the effects of the shadow zones (Figure 2B). LS-WEM also enhances temporal resolution by broadening the frequency spectrum (Figure 2E). Figure 2C and 2D show that LS-WEM balances the wavenumber content and improves the image of the faults and dipping salt flanks.

In addition, LS-WEM converges rapidly to the true solution, reducing the data residuals by 90% in only four iterations (Figure 2F).

We also applied the LS-WEM to a wide azimuth (WAZ) data from the Gulf of Mexico. The results also demonstrate that LS-WEM can deliver superior images compared to the standard migration (Figure 3).

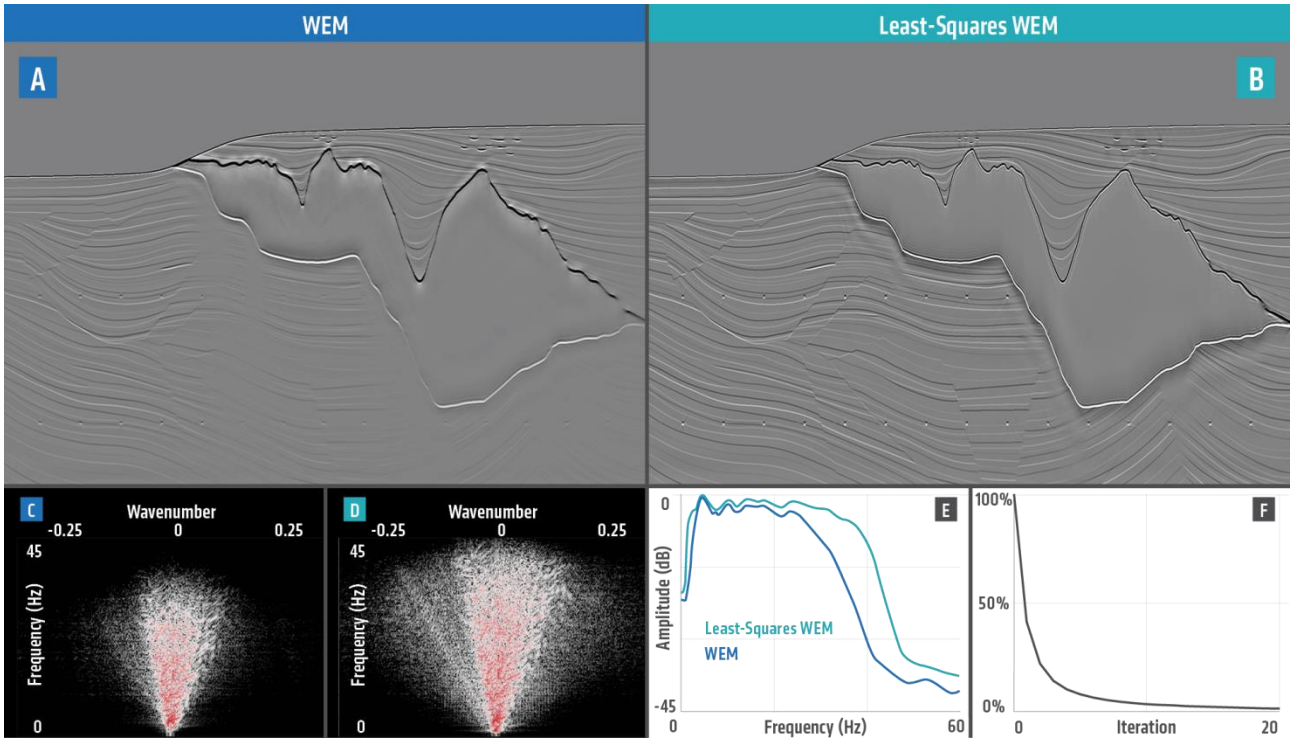

Figure 2: Sigsbee2b 2D synthetic example: (A) WEM image; (B) LS-WEM image; (C) F-K spectrum of WEM; (D) F-K spectrum of LS-WEM; (E) Frequency spectra of WEM and LS-WEM; (F) LS-WEM objective function convergence rate.

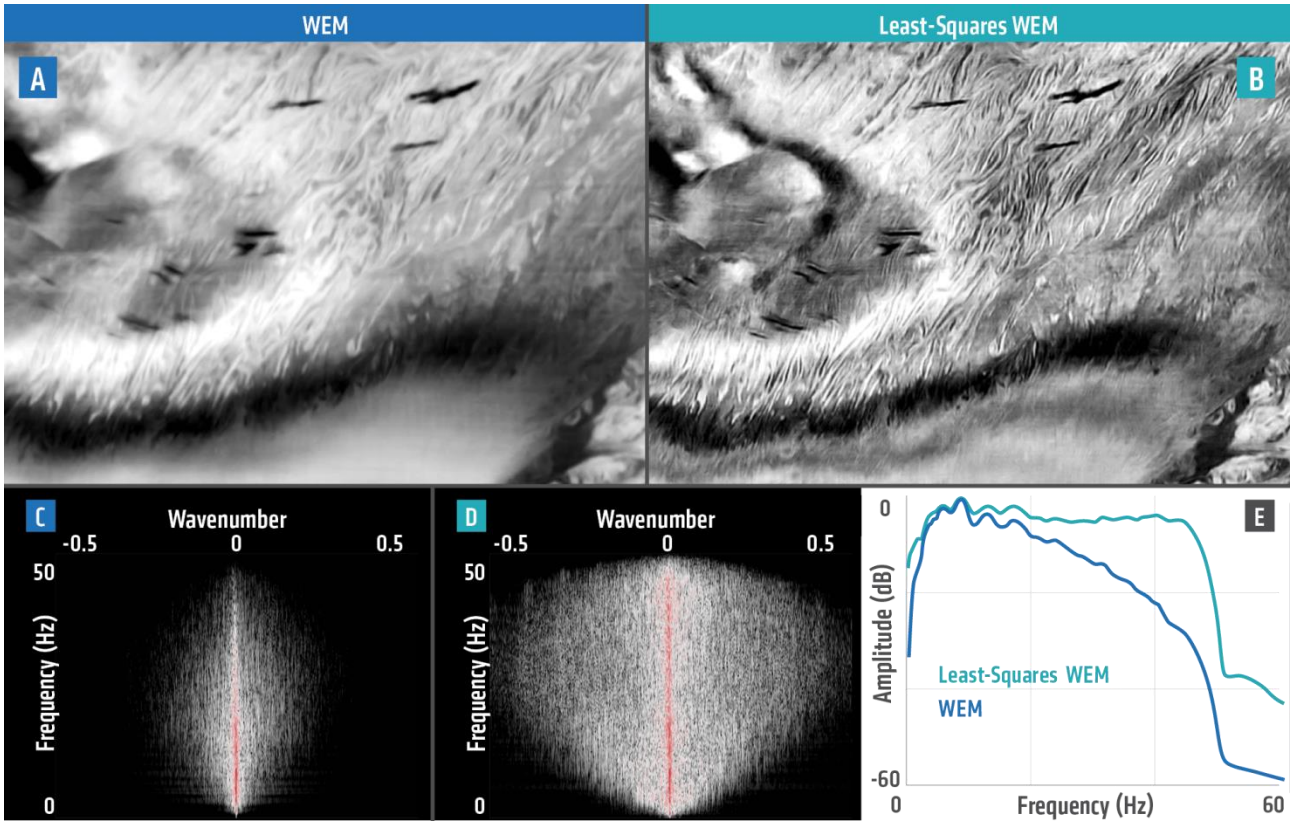

Figure 3: Gulf of Mexico 3D WAZ field data example: (A) Depth slice at 1150 m from WEM; (B) Depth slice at 1150 m from LS-WEM; (C) WEM F-K spectrum; (D) LS-WEM F-K spectrum; (E) Frequency spectra of WEM and LS-WEM.

The image improvements of LS-WEM over the standard migration can be summarized as: reduction of sail line acquisition footprint, better resolution, and improved wavenumber content (Figures 3C, 3D and 3E).

Another example of 3D narrow azimuth (NAZ) data from North Sea further illustrates the advantages of applying LS-WEM to strongly attenuative media with a high resolution velocity model (Korsmo et al., 2017). Figure 4 shows a comparison of the results from WEM and LS-WEM. The standard migration images are corrupted by the acquisition footprint (Figure 4A), a typical problem in shallow water environments. The LS-WEM solution effectively reduces the acquisition footprint leading to a more interpretable image (Figure 4E). LS-WEM also improves the resolution as illustrated in the first two examples. The LS-WEM creates an image with much broader wavenumber content (Figure 4F) compared to WEM (Figure 4B). The improved high wavenumber content enables the LS-WEM solution to produce better images of the fault planes (circled in Figure 4H).

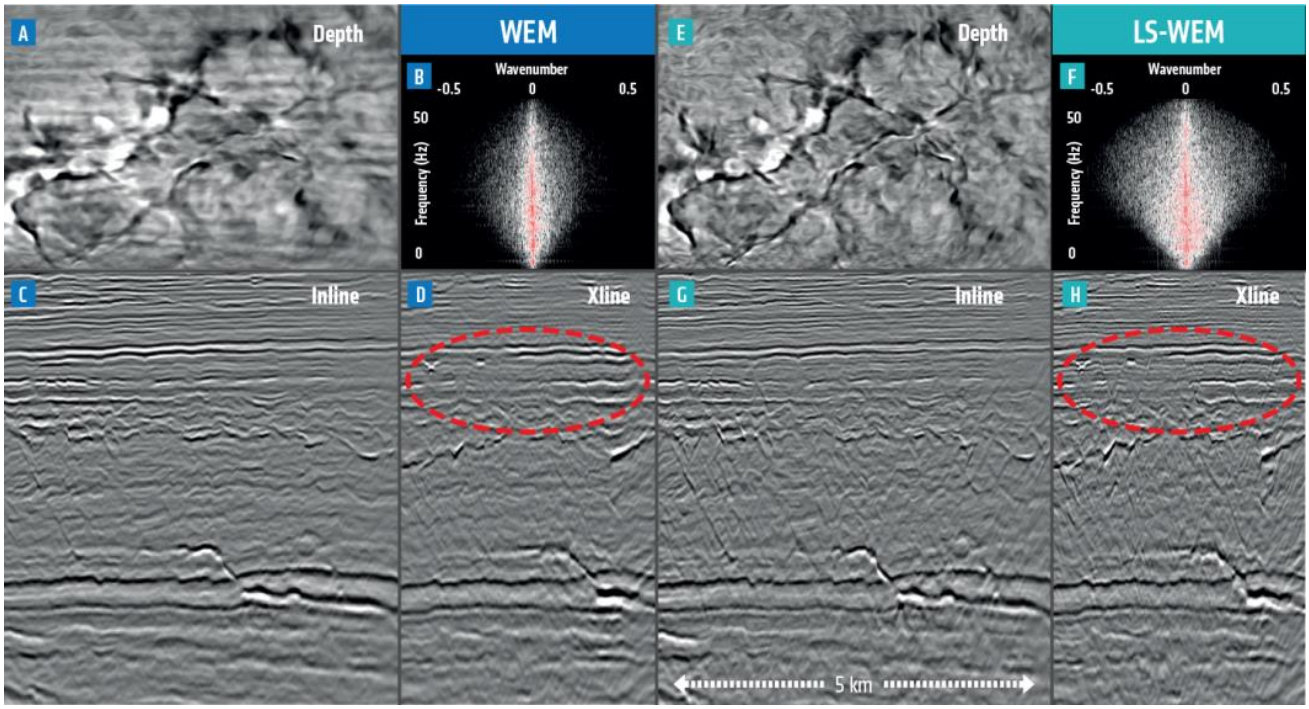

Figure 4: North Sea 3D NAZ field data example. Left: WEM results; Right: LS-WEM results. The depth slice is at 1.8 km.

CONCLUSIONS

We introduce an effective iterative Least-Squares Wave-Equation Migration (LS-WEM) solution for broadband imaging. The Least-Squares Migration is implemented using a one-way wave-equation wavefield propagator that is able to fully utilize both the broader seismic bandwidth and the high-resolution velocity information from FWI. Our implementation combines the one-way extrapolator with fast linear inversion solvers into an efficient migration inversion system. LS-WEM applications to both synthetic and field data demonstrate its ability to generate high-resolution images with better balanced amplitudes, broader frequency bandwidth and larger wavenumber content.

ACKNOWLEDGMENTS

The authors thank PGS for permission to publish this work and for the approval to show the PGS MultiClient Gulf of Mexico data. We are also grateful to Aker BP for permission to publish the North Sea results. Furthermore, we thank Øystein Korsmo and Grunde Rønholt for their support and valuable discussions during the North Sea project.

REFERENCES

Korsmo, Ø., O. J. Askim, Ø. Runde, and Rønholt, G., 2017, High fidelity velocity model building, imaging and reflectivity inversion - A case study over the Viking Graben area, Norwegian North Sea: EAGE Extended Abstracts, Tu A2 13.
Nemeth, T., C. Wu, and Schuster, G., 1999, Least-squares migration of incomplete reflection data: Geophysics, 64, 208–221.
Prucha, M., and Biondi, B., 2002, Subsalt event regularization with steering filters: SEG Expanded Abstracts, 922–925.
Schuster, G., 1993, Least-squares crosswell migration: SEG Expanded Abstracts, 110–113.
Valenciano, A.A., Chemingui, N., Whitmore, D., and Brandsberg-Dahl, S., 2011, Wave equation migration with attenuation compensation: EAGE Extended Abstracts, G008.